Operational Modal Analysis with a 3D Laser Vibrometer without External Reference

Simon Marwitz and Volkmar Zabel,
Institute of Structural Mechanics, Faculty of Civil Engineering, Bauhaus-University Weimar,
Marienstraße 15, 99421 Weimar, Germany

ABSTRACT

The use of Scanning Laser Doppler Vibrometers (SLDV) is a common practice in the context with modal analysis. 3D SLDV have been used with classical experimental modal analysis for several years. In this case, three laser heads which simultaneously point to the same location are used and an additional input reference signal is required to combine the results of consecutive records. In operational modal analysis the input reference signal is replaced by an output reference signal, which may be obtained, for example, from an additional vibrometer or accelerometer.

Alternatively, if a 3 dimensional laser vibrometer is used, one of the three laser heads can be used to provide a reference signal for the other two heads, which can then position their laserbeams independently. However, this requires an appropriate post-estimation method for the transformation of 3D local skew coordinates since the common, built-in routines of commercially available 3D SLDV perform the respective coordinate transformation directly on the simultaneously acquired time series.

In the presented study a respective algorithm has been developed and applied to measured vibration data. For the modal identification the SSI cov/ref algorithm and three different merging strategies have been employed.

Keywords: 3D Scanning Laser Vibrometer, 3D SLDV, coordinate transformation, operational modal analysis, OMA, reference signals

1 Introduction

Laser Doppler Vibrometers (LDV) are widely used for noncontact measurement of vibrations, mainly under laboratory conditions. They provide several advantages over accelerometers that are typically used for vibration measurements. The most prominent is probably the elimination of additional mass loading effects on the dynamic behavior of the structure under test. Scanning LDV can position the laser beam onto different points of a structure automatically and thus speed up the process of multi-point measurements significantly. However, an LDV is limited to measuring vibrations along the direction of the laser beam. 3D SLDV combine 3 laser scan heads, that are placed in different locations and direct their laser beams simultaneously to the same point on a test structure. Vibrations in the Cartesian spatial directions can then be computed for each point of measurement. To combine the multiple single-point measurements, an input or an output reference signal is needed.

In operational modal analysis (OMA) one or more output reference signals are used. Thus, the input or excitation of the structure needs not to be known, which eliminates the demand for any loading device connected to the structure, that might influence the dynamic behavior. Over the years, several methods for the analysis of OMA measurements have been developed. Most of them are adapted from traditional input-output modal analysis. Among the most established methods are the stochastic subspace identification (SSI) modal estimation algorithms with the covariance-driven and the data-driven versions. They originate from system realization theory [5] and are used for the identification of a stochastic state-space model, from which the modal parameters can be extracted.

The combination of multiple measurements based on reference signals can be performed in different ways, depending on the modal estimation algorithm that is employed. The three steps usually involved are: modal analysis, rescaling and merging the data. For the reference-based covariance-driven stochastic subspace identification there exist three such algorithms, described in [1] and [3]. They differ in the order in which the aforementioned steps are performed.

As mentioned before, merging of modal components identified from different setups by means of OMA requires at least one output reference signal. If all three laser beams of a 3D SLDV always point at the same time at a single measuring point, this requirement can only be fulfilled by using an additional sensor, which can also be an SLDV. In this study an approach is presented which allows to circumvent the application of additional sensors.

2 Theory

2.1 3D SLDV: Mode Shape Coordinate Transformation

In the course of a series of 3D SLDV measurements, the velocities at each measuring point are recorded succesively. A single laser vibrometer only measures vector components of any vibration along the direction of its laser beams. Therefore, the quantities at each DOF are available in local skew coordinate systems, too. These quantities may be measured vibration time histories or the components of the estimated mode shapes, also known as modal coordinates. For the visual representation of the mode shapes, an appropriate coordinate transformation at each measuring point is necessary. This cannot be done by simple vector addition of the respective quantities.

As the determined quantity $\mathbf{v_i}$ is only a vector component of the actual quantity $\mathbf{v_r}$ in the direction of measurement, any component perpendicular to this direction is unknown. Thus, the effective quantity has to lie on a line or plane perpendicular to $\mathbf{v_i}$, $\mathbf{v}_{\perp,\mathbf{i}}$. This can be represented by the Hesse normal form of a line in $\mathbb{R}^2$ or a plane in $\mathbb{R}^3$

$$\mathbf{v}_{\perp,\mathbf{i}}: \qquad \mathbf{n_i} \cdot \mathbf{r} = d_i \qquad \text{with} \quad \|\mathbf{n_i}\| = 1, \quad d_i \geq 0\,. \tag{1}$$

In this case the normal vector is the normalized quantity and the distance from the origin d_i is simply it's length

$$\begin{aligned} \mathbf{n_i} = \frac{\mathbf{v_i}}{\|\mathbf{v_i}\|}, \quad d_i &= \mathbf{v_i} \cdot \mathbf{n_i} \\ &= \|\mathbf{v_i}\|\,. \end{aligned} \tag{2}$$

This holds at any DOF for quantity $\mathbf{v_i}$ with $i = 1,2,3$ (number of measurement directions or scan heads). The intersection point of the lines or planes $\mathbf{v_r}$ can be found by solving the linear system of equations with respect to the components of $\mathbf{r}$.

The principle of such a transformation can be shown clearly in the planar case (see Fig. 1a), where $\mathbf{v_i} : [a_i, b_i]^\intercal$ with $i = 1,2$ and $\mathbf{v_r} : [x_r, y_r]^\intercal$. The solution is found e.g. by applying Cramer's rule

$$x_r = \frac{-\Delta_x}{\Delta}, \quad y_r = \frac{-\Delta_y}{\Delta}, \quad \text{with} \quad \Delta = \begin{vmatrix} a_1 & b_1 \\ a_2 & b_2 \end{vmatrix}, \quad \Delta_x = \begin{vmatrix} -d_1^2 & b_1 \\ -d_2^2 & b_2 \end{vmatrix} \text{ and } \quad \Delta_y = \begin{vmatrix} a_1 & -d_1^2 \\ a_2 & -d_2^2 \end{vmatrix}. \tag{3}$$

It has to be mentioned, though, that if the amplitude of either of the quantities $\mathbf{v_i}$ vanishes (e.g. the direction of vibration is perpendicular to the laser beam), the solution fails.

In the 3-dimensional case the DOFs are extended by another dimension $\mathbf{v_i} : [a_i, b_i, c_i]^\intercal$ and the system of linear equations by a third variable, $\mathbf{v_r} : [x_r, y_r, z_r]^\intercal$. The actual derivation of the procedure holds for any dimension ≥ 2. An intuitive representation of the procedure would be to find the intersection point v_r of three planes $\mathbf{v}_{\perp,\mathbf{i}}$ in $\mathbb{R}^3$ (see Fig. 1b). Again, the application of Cramer's rule (under the condition of non-zero amplitudes of the respective quantities) leads to the following solution

$$x_r = \frac{-\Delta_x}{\Delta}, \quad y_r = \frac{-\Delta_y}{\Delta}, \quad z_r = \frac{-\Delta_z}{\Delta} \tag{4}$$

with

$$\Delta = \begin{vmatrix} a_1 & b_1 & c_1 \\ a_2 & b_2 & c_2 \\ a_3 & b_3 & c_3 \end{vmatrix}, \quad \Delta_x = \begin{vmatrix} -d_1^2 & b_1 & c_1 \\ -d_2^2 & b_2 & c_2 \\ -d_3^2 & b_3 & c_3 \end{vmatrix}, \quad \Delta_y = \begin{vmatrix} a_1 & -d_1^2 & c_1 \\ a_2 & -d_2^2 & c_2 \\ a_3 & -d_3^2 & c_3 \end{vmatrix}, \quad \Delta_z = \begin{vmatrix} a_1 & b_1 & -d_1^2 \\ a_2 & b_2 & -d_2^2 \\ a_3 & b_3 & -d_3^2 \end{vmatrix}. \tag{5}$$

Finally, it should be noted that at each point of measurement, the laser beams intersect at different angles. Hence the local skew coordinate system is different at each point. Regarding the solution of the linear systems of equations, due to the nature of 3D

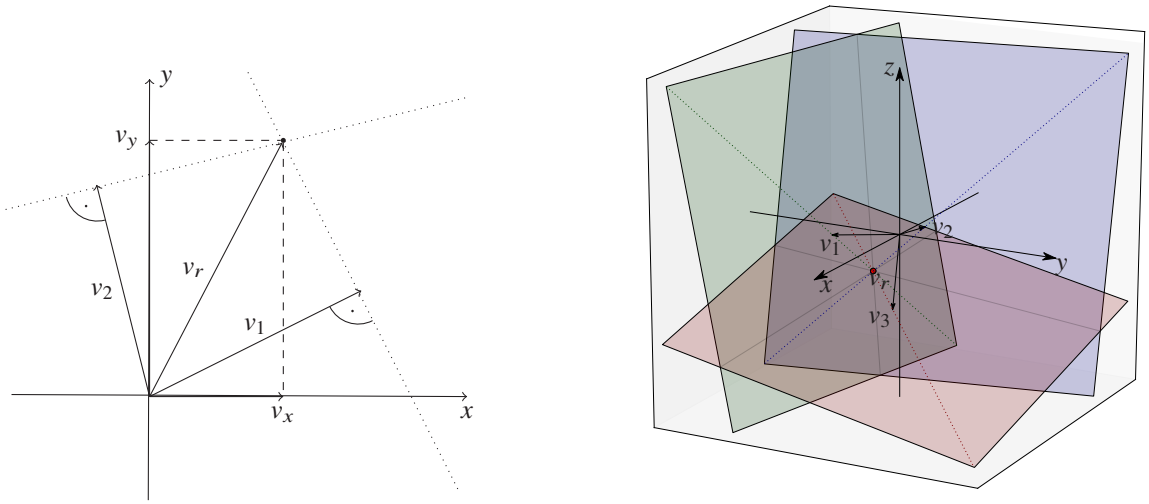

(a) . . . in the x-y-plane **(b)** . . . in 3D Space

Figure 1 3D transformation of modal coordinates

SLDV measurements parallel lines or planes should not occur, but there may be cases where either of the quantities vanishes. A three-dimensional transformation is then reduced to a planar case in the plane of the remaining DOFs.

In this study only the quantities at each DOF obtained as parts of estimated mode shapes were used. These are mostly real valued, but there are cases where mode shapes exhibit significant relative phase angles, i.e. the amplitudes are complex valued. It has been verified by a parametric study that the proposed algorithm can be successively applied to complex valued quantities and that the phase angles are transformed appropriately. Nevertheless a mathematical proof is yet to be provided.

2.2 Operational Modal Analysis: Stochastic Subspace Identification

The use of stochastic subspace identification techniques is a well known method in operation modal analysis. The main algorithm and equations of the reference-based, covariance-driven stochastic subspace identification that has been used in this study, will be briefly recalled as given in [4].

By introducing the state vector

$$\mathbf{x}(t) = \begin{bmatrix} \mathbf{y}(t) & \dot{\mathbf{y}}(t) \end{bmatrix}^{\mathsf{T}} \tag{6}$$

into the general equation of motion of a multi degree of freedom, linear, time-invariant system, a state-space model can be derived. Following the discretization and replacing the unknown input terms by stochastic white noise terms $\mathbf{w_k}$ and $\mathbf{v_k}$ a discrete time stochastic state-space model is obtained

$$\begin{aligned} \mathbf{x}_{k+1} &= \mathbf{A}_d \mathbf{x}_k + \mathbf{w}_k \\ \mathbf{y}_k &= \mathbf{C}\mathbf{x}_k + \mathbf{v}_k \,, \end{aligned} \tag{7}$$

where $\mathbf{A}_d$ denotes the state matrix and $\mathbf{C}$ the output matrix, respectively. In the covariance-driven stochastic subspace identification such a state-space model is estimated from measured time series. The following expected values can be obtained from the state-space model

$$\begin{aligned} \mathbf{G}^{ref} &= \mathrm{E}\left[\mathbf{x}_{k+1} \quad \mathbf{y}_k^{ref\,\mathsf{T}}\right], \qquad \mathbf{R}_i^{ref} = \mathrm{E}\left[\mathbf{y}_{k+i} \quad \mathbf{y}_k^{ref\,\mathsf{T}}\right] \\ &\qquad\qquad\qquad\qquad = \mathbf{C}\mathbf{A}^{i-1}\mathbf{G}^{ref} \,. \end{aligned} \tag{8}$$

Here $\mathbf{G}^{ref}$ denotes the next-state output covariance matrix and $\mathbf{R}_i^{ref}$ the output-covariance matrix at time-lag i. In the case of reference-based stochastic subspace identification these matrices are computed only between the output-channels and selected reference channels Equation 8 is especially important, as the covariances can be estimated directly from the recorded timeseries.

Several covariance matrices at ascending time lags i are arranged into a block-Toeplitz-Matrix

$$\hat{\mathbf{T}}_{1|i}^{ref} = \begin{bmatrix} \hat{\mathbf{R}}_{i}^{ref} & \hat{\mathbf{R}}_{i-1}^{ref} & \dots & \hat{\mathbf{R}}_{1}^{ref} \\ \hat{\mathbf{R}}_{i+1}^{ref} & \hat{\mathbf{R}}_{i}^{ref} & \dots & \hat{\mathbf{R}}_{2}^{ref} \\ \vdots & \vdots & \ddots & \vdots \\ \hat{\mathbf{R}}_{2i-1}^{ref} & \hat{\mathbf{R}}_{2i-2}^{ref} & \dots & \hat{\mathbf{R}}_{i}^{ref} \end{bmatrix} \tag{9}$$

where $\hat{\circ}$ denotes "estimate". The matrix $\mathbf{T}_{1|i}^{ref}$ can also be written in terms of the state variables

$$\begin{aligned} \mathbf{T}_{1|i}^{ref} &= \begin{bmatrix} \mathbf{C} \\ \mathbf{CA} \\ \vdots \\ \mathbf{CA}^{i-1} \end{bmatrix} \begin{bmatrix} \mathbf{A}^{i-1}\mathbf{G}^{ref} & \dots & \mathbf{AG}^{ref} & \mathbf{G}^{ref} \end{bmatrix} \\ &= \mathbf{O}_i \boldsymbol{\Gamma}_i \,, \end{aligned} \tag{10}$$

$\mathbf{O}_i$ and $\boldsymbol{\Gamma}_i$ denote the observability matrix and controllability matrix, respectively. A singular value decomposition

$$\hat{\mathbf{T}}_{1|i}^{ref} = \begin{bmatrix} \mathbf{U}_1 & \mathbf{U}_2 \end{bmatrix} \begin{bmatrix} \mathbf{S}_1 & \mathbf{0} \\ \mathbf{0} & \mathbf{S}_2 \end{bmatrix} \begin{bmatrix} \mathbf{V}_1^\intercal \\ \mathbf{V}_2^\intercal \end{bmatrix} \tag{11}$$

and the truncation of singular values at the desired model order is employed to obtain the matrices

$$\mathbf{O}_i = \mathbf{U}_1 \mathbf{S}_1^{0.5} \,, \quad \text{and} \quad \boldsymbol{\Gamma}_i = \mathbf{S}_1^{0.5} \mathbf{V}_1^\intercal . \tag{12}$$

The output matrix $\mathbf{C}$ can be extracted from the first l rows of $\mathbf{O}_i$, with l being the number of analyzed channels. There exist several alternatives for the computation of the state matrix $\mathbf{A}$. One common method is given by

$$\mathbf{A} = \mathbf{O}_i^{\uparrow\,\dagger} \mathbf{O}_i^{\downarrow} \tag{13}$$

where $\circ^\dagger$ denotes a pseudoinverse. $\mathbf{O}_i^{\uparrow}$ and $\mathbf{O}_i^{\downarrow}$ are obtained by removing the last and the first block rows of $\mathbf{O}_i$, respectively. An eigendecomposition of the state matrix $\mathbf{A}$ leads to the eigenvalues $\boldsymbol{\Lambda} = \mathrm{diag}(\lambda_r)$ and eigenvectors $\boldsymbol{\Psi}$, which occur in complex conjugate pairs. The natural frequencies f_r and damping values ζ_r can be computed from the eigenvalues

$$\mu_r = \frac{\ln(\lambda_r)}{\Delta t}, \quad f_r = \frac{|\mu_r|}{2\pi}, \quad \zeta_r = \frac{\mathrm{Re}(\mu_r)}{|\mu_r|} \,. \tag{14}$$

Multiplying the matrix of eigenvectors with the output matrix yields the mode shape matrix

$$\boldsymbol{\Phi} = \mathbf{C}\boldsymbol{\Psi} \,. \tag{15}$$

2.3 Multi-Setup Merging Strategies

In operational modal analysis it is frequently required to carry out measurements on multiple points of a structure in order to obtain an adequate representation of the mode shapes of a structure. Limitations regarding the number of available sensors may apply and consequently, consecutive measurements using different sensor location setups are performed. In order to recombine these afterwards, one or more common output reference sensors, which remain at the same position throughout all setups, are used. [3] and [1] introduce three different strategies for data merging of multi-setup measurements using reference sensor data. These approaches mainly differ in the order of the steps: modal analysis, data merging and data re-scaling (see Figure 2).

The classic approach, termed PoSER (Post Separate Estimation Re-scaling), is the common practice in operational modal analysis. Each setup $j = 1 \dots n_s$ is processed individually to obtain the modal parameters f_r^j, ζ_r^j and mode shapes $\boldsymbol{\phi}_r^j$ for the one mode r. The separate, incomplete mode shapes are then combined and rescaled relative to measurement j^*

$$\boldsymbol{\phi}_s = \begin{bmatrix} \boldsymbol{\phi}_r^{ref,j*} \\ \boldsymbol{\phi}_r^{m,j*} \\ \alpha_r^{j*,1} \boldsymbol{\phi}_r^{m,1} \\ \vdots \\ \alpha_r^{j*,n_s} \boldsymbol{\phi}_r^{m,n_s} i \end{bmatrix} \quad \text{with} \quad \alpha_r^{j*,j} = \left(\boldsymbol{\phi}_r^{ref,j*\mathrm{H}} \boldsymbol{\phi}_r^{ref,j*} \right)^{-1} \boldsymbol{\phi}_r^{ref,j*\mathrm{H}} \boldsymbol{\phi}_r^{ref,j} \,, \tag{16}$$

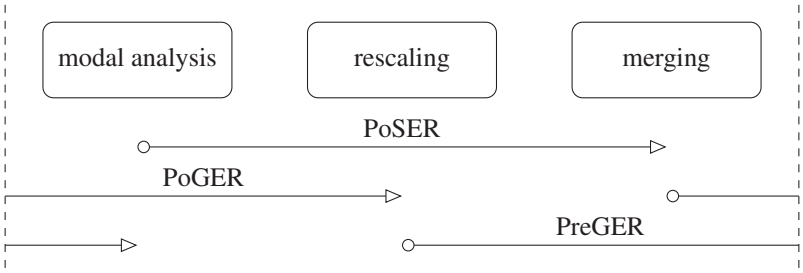

Figure 2 Order of steps for the three merging strategies for SSI cov/ref

where $\circ^r$ and $\circ^m$ denote reference channels and moving channels, respectively and $\circ^{\mathrm{H}}$ denotes a conjugate transpose. Especially if a large number of DOFs need to be included, this approach requires many measurements to be processed individually.

The second merging approach, termed PoGER (Post Global Estimation Re-scaling), aims at reducing the workload by processing all setups together. However this can only be done if the tested structure exhibits linear behavior (e.g. no frequency shifts due to temperature, loading amplitudes, etc.). The reference sensors, whose signals are used to compute the covariances are required to stay on the same location in all setups. The reference-based covariance matrices are stacked block-row-wise

$$\hat{\mathbf{R}}_i^{all} = \begin{bmatrix} \hat{\mathbf{R}}_i^1 \\ \hat{\mathbf{R}}_i^2 \\ \vdots \\ \hat{\mathbf{R}}_i^{n_s} \end{bmatrix} . \tag{17}$$

These total covariance matrices for different time lags i are then assembled into a block-Toeplitz-matrix, that is used for system identification and modal analysis, as described in the previous section. The resulting mode shapes $\boldsymbol{\phi}_r^j$ come out stacked in the same manner. Each setup's part has to be rescaled separately similarly to the PoSER approach, equation (16), and the reference channels are removed afterwards.

To overcome the limitations regarding the linear behavior of the tested structures, a third approach, termed PreGER (Pre Global Estimation Re-scaling), was introduced. A detailed derivation of the procedure is given in [3], here it is briefly described. In contrast to the other approaches, rescaling is now applied to the covariance matrices, before merging the setups. The scaling matrices are obtained in state-space by means of a common controllability matrix, which reflects the differences in excitation between all setups. In order to compute this matrix, the covariance-matrices of only the reference channels $\hat{\mathbf{R}}_i^{j,ref}$ are built for all setups j and stacked block-column-wise

$$\hat{\mathbf{R}}_i^{all,ref} = \begin{bmatrix} \hat{\mathbf{R}}_i^{1,ref} & \dots & \hat{\mathbf{R}}_i^{n_s,ref} \end{bmatrix} . \tag{18}$$

Thus the next-state covariance matrices turn out to be stacked in the same manner and can be obtained from the factorization property

$$\mathbf{R}_i^{all,ref} = \mathbf{C}^{ref}\mathbf{A}^{i-1}\mathbf{G}^{all} \quad \text{with} \quad \mathbf{G}^{all} = \begin{bmatrix} \mathbf{G}^1 & \dots & \mathbf{G}^{n_s} \end{bmatrix} . \tag{19}$$

A common controllability matrix $\boldsymbol{\Gamma}_i^{all}$ can then be computed by means of a singular value decomposition of a block-Toeplitz matrix assembled from the stacked covariance matrices equation (12). Recalling the definition from equation (**??**) and considering equation (19), the single-setup controllability matrices $\boldsymbol{\Gamma}^j$ can be extracted from the common controllability matrix by selecting the appropriate row-columns. Fitting the single matrices with respect to the controllability matrix of a selected setup j^*, yields the rescaling matrices $\overline{\boldsymbol{\alpha}}^{j,j*}$

$$\boldsymbol{\Gamma}^j = \boldsymbol{\Gamma}^{j*}\overline{\boldsymbol{\alpha}}^{j,j*} . \tag{20}$$

The Moore-Penrose pseudoinverse † can be used to provide a least-squares solution to this overdetermined linear system of equations

$$\overline{\boldsymbol{\alpha}}^{j,j*} = \boldsymbol{\Gamma}^{j\,\dagger}\boldsymbol{\Gamma}^{j*} . \tag{21}$$

The block-Toeplitz matrices of covariance matrices built from the moving sensor data can be rescaled with the obtained scaling factors

$$\overline{\mathbf{T}}^{j,m} = \mathbf{T}^{j,m}\overline{\boldsymbol{\alpha}}^{j,j*} . \tag{22}$$

Block-row-wise interleaving of the rescaled block-Toeplitz matrices yields a global block-Toeplitz matrix that can be used to apply the system identification and modal analysis, as described in the previous section.

3 Proposed Approach

With commercially available 3D SLDV, single-point measurements with pre-estimation coordinate transformations are compulsory. That means, vibration time histories or power spectral densities are transformed at the time of recording to be available in the tested structure's Cartesian coordinates. In order to combine consecutive single-point measurements, an additional input or output reference signal is required. In both cases this requires connecting sensors or excitation devices to the structure. These may influence the dynamic behavior, especially of lightweight structures. To circumvent this interaction an additional LDV may be used to provide a reference signal, which is costly and requires additional effort in terms of synchronized data acquisition.

The derivation of a post-estimation coordinate transformation approach in the presented study opens the possibility for multi-point measurement schemes. Hence, single-point measurements are not required anymore and the time histories can be used as measured by the single scan heads. In a multi-point measurement scheme, each laser beam is directed toward a different measuring point. In a series of consecutive measurements each measuring point is scanned by each scan head, once. Merging the modal results of all measurements yields complete mode shapes. Nevertheless, these are available in local skew coordinates where the axes are pointing toward the locations of the three scan heads. These local coordinate systems are different for each measuring point and have to be transformed into global Cartesian coordinates for visualization and comparison purposes.

Taking it one step further, this opens the possibility to use each scan head to provide a reference signal for the remaining scan heads, respectively. Figure 3 shows the general procedure. A multi-point measurement scheme, consisting of multiple setups is partitioned into three sets of setups. In each set, a different scan head provides the reference signals. An additional "all-reference" measurement is required, where all scan heads direct their laser beams to the respective reference positions at the same time. Subsequently, the modal data of all setups is merged in a two-step approach. In the first step the setups of each set are merged, using one of the three presented merging strategies. In the second step, the three sets are merged using the PoSER approach with aid of the "all-reference" measurement. Finally, the transformation of the mode shapes from local skew coordinates into global Cartesian coordinates is performed.

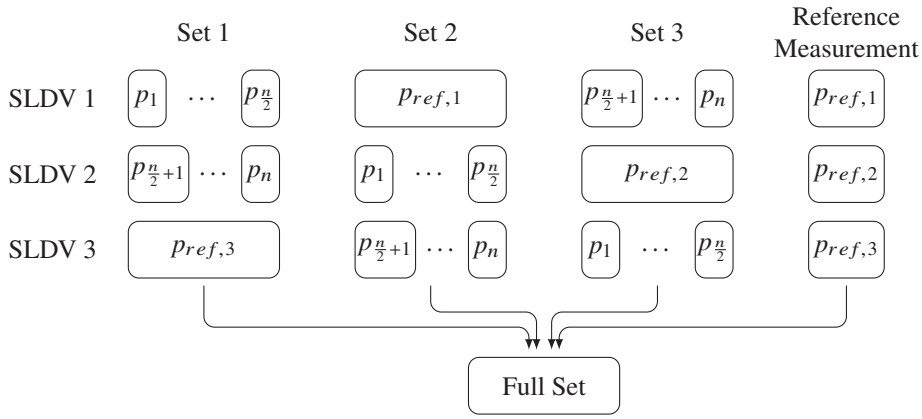

Figure 3 Procedure of measurement according to the proposed approach, with p_i: measuring point i; n: total number of measuring points and $p_{ref,j}$: reference point for scan head j

As with every other type of multi-setup measurement, the key for good results lies the selection of appropriate reference sensor positions. The typical requirements for reference sensor positions arise from the need for a sufficient representation of each mode of interest in the recorded signal. Therefore, the nodal points of any mode of vibration should be avoided. Furthermore, under consideration of the expected excitation, each mode of vibration should create acceptably high amplitudes at the selected locations. A sufficient number of reference locations should be chosen to account for all spatial directions of vibrations. In the proposed approach another requirement stems from the inability of the LDV to measure vibrations perpendicular to the direction of the laser beam. Therefore the measurement directions cannot be arbitrarily chosen, as e.g. in the case of accelerometers,

but are predetermined by the positions of the scan heads relative to the tested structure. In summary, each scan head needs a reference point that shows sufficient amplitudes in each mode of vibration and in the respective measurement direction. Typically a numerical model is created for a preliminary modal analysis that can be used to determine adequate reference positions for each scan head. Alternatively, a preliminary measurement can be used for this purpose.

4 Application

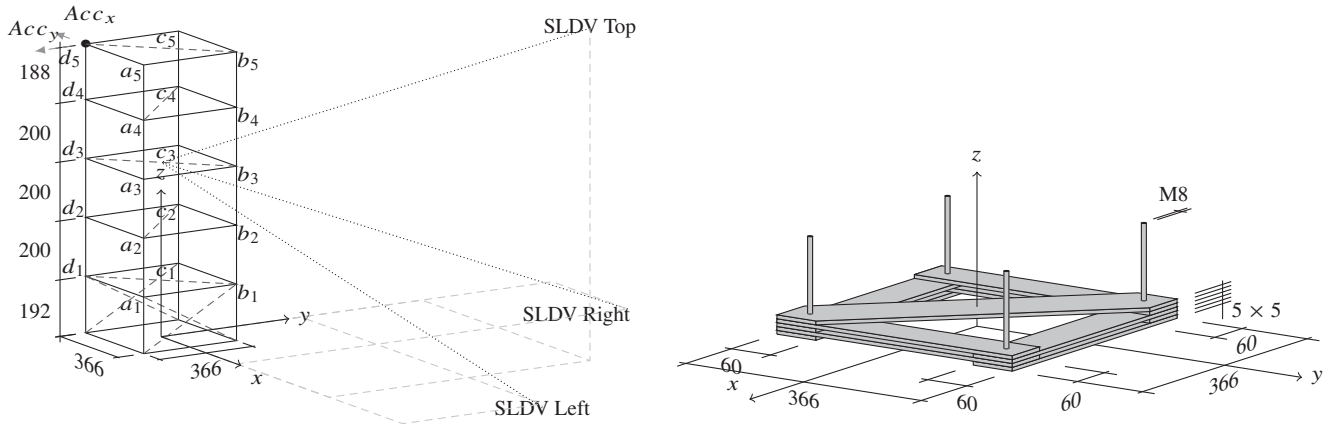

(a) Overview, labeling of points.

(b) Detailed view of one platform of the tower.

Figure 4 3D view of the test structure with dimensions in mm.

The proposed approach was applied using a commercial 3D SLDV (Polytec PSV 400-3D) that is available at the Bauhaus University in Weimar, Germany. A small-scale, tower-like, skeletal structure was chosen for the tests, as it vibrates in at least two directions and can be tested in the laboratory. Figure 4 shows a 3D view of the structure. The columns are made of steel threaded rods and the single platforms consist of flat steel bars that are connected to form a relatively stiff slab. Additional bracing can be attached between all levels. In this case the lowest storey was braced in y-direction to avoid the coupling of modes in the horizontal directions.

In general, when conducting SLDV measurements there has to exist a line of sight between the SLDV and the measuring point. In the case of a 3D SLDV, only the points that satisfy this requirement for all scan heads can be used for measurements. Thus it is clear, that only a part of a 3D structure can be included without changing the positions of the scan heads (or using special mirrors). To maximize the number of available measuring points the structure was positioned diagonally towards the plane of the three scan heads, such that one corner faces the SLDV at the top. Two additional accelerometers were mounted to the structure, which were used for conducting a preliminary measurement but left in place unused afterwards to avoid mass change effects. The exact positioning of the structure and the three scan heads are also illustrated in Figure 4.

4.1 Experimental Setup

A first insight into the dynamic behavior of the structure was gained from a numerical FEM analysis. Based on these results, the positions of the three scan heads were chosen and reference accelerometers were placed on measuring point d_5 in both horizontal directions. The accelerometers were used for a preliminary reference measurement that was conducted using single-point measurements with pre-estimation coordinate transformation, in the way that is intended by the manufacturer of the 3D SLDV.

The final experimental setup for the application of the proposed approach was created based on the results of the preliminary measurement. The reference locations were chosen to be at the same point, namely point c_5, for all scan heads in order to reduce influencing factors on the final results. A sufficient representation of all modes of interest in each single setup was the

aim for the creation of moving point combinations. The resulting 22 setups are shown in figure 5. An independent positioning of the laser beams was achieved by utilizing the macro programming capabilities of the software provided by the manufacurer.

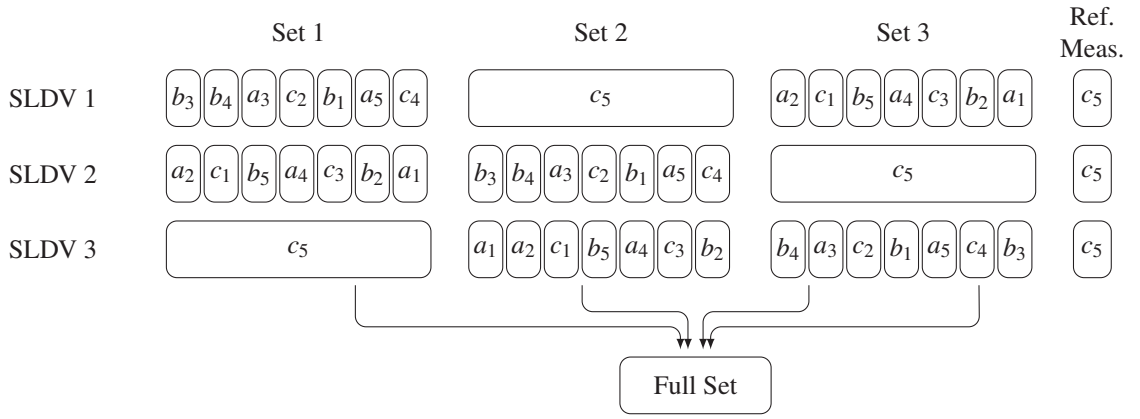

Figure 5 All setups used in the experimental study, refer to Figure (4) for labels of the measuring points

Another aim of the experimental application was the comparison and evaluation of the performance of the three multi-setup merging strategies presented in section 2.3. Therefore ambient excitation (i.e. non-stationary power spectrum) was required and achieved through the use of two moving ventilators, exciting the structure aerodynamically.

The vibration velocities were recorded at a sampling frequency of 512 Hz for a duration of 256 s. However for the analysis the data was decimated by a factor of 2. The analysis was performed with an own implementation of the SSI cov/ref algorithm, with parameters $i = 200$ (number of block rows) and $n_{max} = 200$ (maximum model order). After the manual selection of stable poles for each mode of interest, the setups were merged following the PoSER strategy. In the case of 22 setups this is a time consuming process. To evaluate the performance and accuracy of the other two merging strategies, those were applied as well. In that case all setups belonging to one set were merged following the PoGER and PreGER approach, respectively, and subsequently the three sets were merged using the PoSER algorithm. Finally, the coordinates of the mode shapes were transformed to Cartesian coordinates. That allowed not only for the visualization, but also for the comparison with the mode shapes obtained from the preliminary measurement.

4.2 Discussion of Results

As a result of the modal analysis, 14 modes of vibration were identified with varying quality. Figure 6 shows examples of the mode shapes, as identified in the reference measurement. The modal parameters resulting from the measurements following the proposed approach are summarized in table 1.

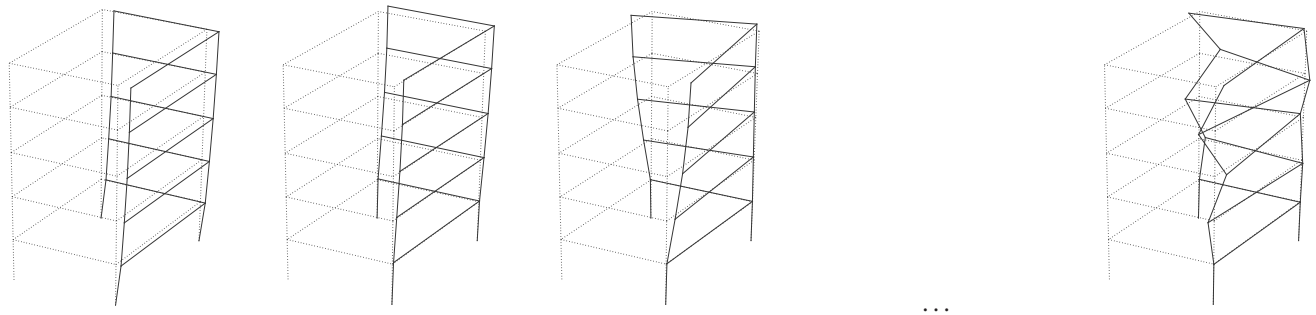

Figure 6 Examples of experimentally identified mode shapes of the test structure.

1: bending x_1	2: bending y_1	3: torsion t_1	4: bending x_2[1]	5: bending x_2	6: bending y_2	7: torsion t_2
$f = 2.20\,\text{Hz}$ $\zeta = 1.3\,\%$	$f = 2.95\,\text{Hz}$ $\zeta = 1.8\,\%$	$f = 4.28\,\text{Hz}$ $\zeta = 0.4\,\%$	$f = 6.95\,\text{Hz}$ $\zeta = 6.6\,\%$	$f = 9.00\,\text{Hz}$ $\zeta = 1.7\,\%$	$f = 11.62\,\text{Hz}$ $\zeta = 1.3\,\%$	$f = 13.78\,\text{Hz}$ $\zeta = 1.5\,\%$
8: bending x_3	9: bending y_3	10: bending x_4	11: torsion t_3	12: longitud. z_1[2]	13: diagonal d_1[3]	14: torsion t_4
$f = 14.15\,\text{Hz}$ $\zeta = 0.4\,\%$	$f = 17.59\,\text{Hz}$ $\zeta = 0.7\,\%$	$f = 18.79\,\text{Hz}$ $\zeta = 0.3\,\%$	$f = 20.94\,\text{Hz}$ $\zeta = 0.2\,\%$	$f = 22.09\,\text{Hz}$ $\zeta = 0.7\,\%$	$f = 22.23\,\text{Hz}$ $\zeta = 0.5\,\%$	$f = 25.53\,\text{Hz}$ $\zeta = 0.1\,\%$

Table 1 All 14 experimentally identified natural frequencies and damping coefficients of the test structure.

However, not every merging strategy led to the identification of all modes of interest. Additionally, the modal parameters showed varying deviations with respect to the reference measurement. Figure 7a shows the frequency deviations for each mode of interest and separately for all merging strategies. In a similar manner the absolute damping values are shown in figure 7b. Here the results obtained from the reference measurement are marked by a dashed horizontal line for comparison. Finally, the modal assurance criterion (MAC) [2, p. 424] of the identified mode shapes was calculated with respect to the mode shapes obtained from the reference measurement, which is shown in figure 7c.

Especially the modes 4, 12 and 13 could not be identified or show high deviations in the respective parameters. A good agreement was reached for most of the bending modes in x-direction (1, 5, 8,10) as well as the torsional modes (3, 7, 11, 14). But a general pattern regarding the identifiability could not be found. Nevertheless, the mode shapes show significant differences, especially if the PreGER merging approach was used. Here the separate identification and subsequent merging (PoSER) leads to the best results, while the PoGER approach is still feasible.

There are several reasons, explaining those differences. First of all, it has to be mentioned that the reference measurement and the measurement following the proposed approach were performed under marginally different boundary conditions. There was an error in the data acquisition during the first run of the second measurement which was not noted until the structure was already moved from its original location and changed structurally. Thus, after restoration, it became apparent that the dynamic behavior of the structure had slightly changed.

Secondly, the merging of several setups is highly dependent on the quality of the reference signals. As a result any inaccuracies in the combined mode shapes lead to major errors during the following 3D transformation. In this case the reference points were chosen to be at the same location for all scan heads. This choice was based upon engineering judgment, but choosing different reference points for each scan head might have resulted in better quality reference signals.

In order to improve the results, several measures are conceivable. The placement of the scan heads relative to the structure could be optimized based on a preliminary experimental and/or numerical modal analysis. Additionally the aerodynamic excitation might not be the best choice for a proper modal analysis. Therefore, different types of excitation could be chosen. As mentioned already the selection of suitable reference points for each scan head could also be based on preliminary and/or numerical studies to further improve the quality of the reference signals. And finally, there was no evaluation of adequacy of the chosen parameters for the data acquisition, the data processing, the stochastic subspace identification algorithm and the selection of stable poles.

5 Conclusion

In the presented study, it was shown, that it is possible to conduct 3D SLDV measurements without any additional input or output reference signal. A post-estimation 3D coordinate transformation algorithm was developed and applied to experimental data. Three different merging strategies were evaluated in terms of their applicability and accuracy in the context of the reference-based, covariance-driven stochastic subspace identification method.

In this study, the classical PoSER approach led to the best results, while the PreGER approach was not satisfying. The PoGER

[1]Mode 4 could only be completely identified using the PoGER merging approach.
[2]Mode 12 could not be identified in all setups and is therefore incomplete.
[3]Mode 13 could only be completely identified using the PoGER merging approach.

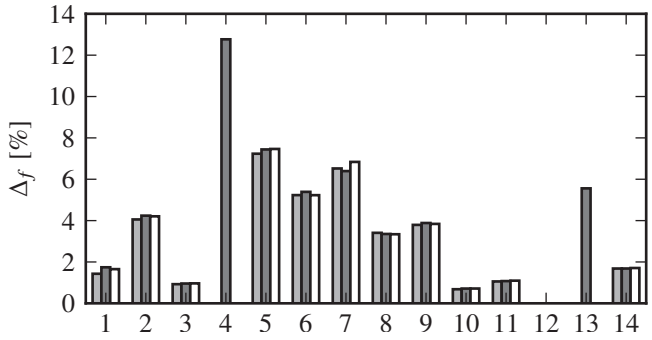

(a) Frequency differences in percent relative to the reference measurement.

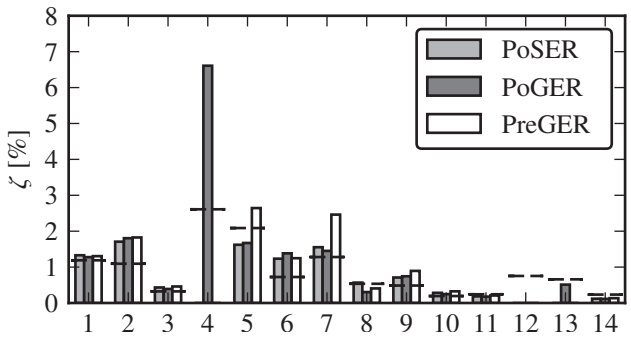

(b) Absolute damping values. Reference measurement is marked by a dashed horizontal line.

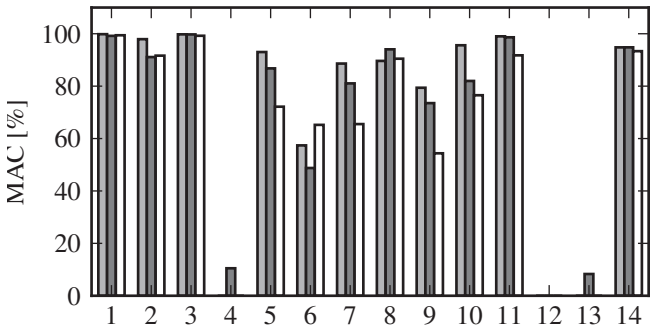

(c) Modal Assurance Criterion of identified modeshapes with respect to the reference measurement.

Figure 7 Manually selected modal parameters for 14 modes of vibration that were chosen. No bar indicates that the respective mode could not be identified. The comparison of the three merging strategies is based on the same experimental data.

merging approach was found to be a good compromise between accuracy of results and time expenditure. The proposed 3D coordinate transformation algorithm was shown to be applicable, but prone to errors. In particular any inaccuracy that occured during merging led to large errors after the 3D coordinate transformation. However, these deficiencies seem to be mainly related to the selection of suitable reference points.

For further research it is recommended to evaluate the proposed approach using a different test structure and/or different modal analysis methods. Additionally, it should be generally possible to use two and more single SLDV to imitate commercial 3D SLDV. However, synchronized demodulation of the doppler signal and data acquisition must be tackled.

References

[1] Döhler, M., Reynders, E., Magalhaes, F., Mevel, L., Roeck, G. D., and Cunha, A. Pre-and post-identification merging for multi-setup oma with covariance-driven ssi. In *28th International Modal Analysis Conference* (2010), Springer New York.

[2] Ewins, D. J. *Modal testing: theory, practice, and application*, vol. Mechanical engineering research studies. Research Studies Press, 2000.

[3] Mevel, L., Basseville, M., Benveniste, A., and Goursat, M. Merging sensor data from multiple measurement set-ups for non-stationary subspace-based modal analysis. *Journal of Sound and Vibration 249*, 4 (2002), 719–741.

[4] Peeters, B., and de Roeck, G. Reference-based stochastic-subspace identification for output-only modal analysis. *Mechanical Systems and Signal Processing* (1999).

[5] Rainieri, C., and Fabbrocino, G. *Operational Modal Analysis of Civil Engineering Structures - An Introduction and Guide for Applications*. Springer, Berlin, Heidelberg, 2014.